

Reverse Doppler effect in backward spin waves scattered on acoustic waves

A. V. Chumak,¹ P. Dhagat,² A. Jander,² A. A. Serga,¹ and B. Hillebrands¹¹Fachbereich Physik and Forschungszentrum OPTIMAS,

Technische Universität Kaiserslautern, 67663 Kaiserslautern, Germany

²School of Electrical Engineering and Computer Science, Oregon State University, Corvallis, OR, USA
(Dated: February 22, 2024)

We report on the observation of reverse Doppler effect in backward spin waves reflected off surface acoustic waves. The spin waves are excited in a yttrium iron garnet (YIG) film. Simultaneously, acoustic waves are also generated. The strain induced by the acoustic waves in the magnetostrictive YIG film results in the periodic modulation of the magnetic anisotropy in the film. Thus, in effect, a travelling Bragg grating for the spin waves is produced. The backward spin waves reflecting off of this grating exhibit a reverse Doppler shift: shifting down rather than up in frequency when reflecting off of an approaching acoustic wave. Similarly, the spin waves are shifted up in frequency when reflecting from receding acoustic waves.

PACS numbers: 75.30.Ds, 76.50.+g, 85.70.Ge

The Doppler effect (or Doppler shift) is a well known phenomenon in which a wave emitted from a moving source or reflected off of a moving boundary is shifted in frequency [1, 2]. When the source or reflector is approaching the receiver, the frequency of received wave is shifted up in frequency. Similarly, the frequency shifts down if the source or reflector is moving away from the observer. The effect is widely used in radar systems, laser vibrometry and astronomical observations.

In, so called, left-handed media [3] the reverse (or anomalous) Doppler effect occurs [4, 5, 6, 7, 8]. This effect is characterized by the opposite frequency shift: waves reflect from an approaching boundary with lower frequency. Conversely, waves reflect from a receding boundary with higher frequency. The explanation for the reversal Doppler shift is that in left-handed media, the group and phase velocities of the waves are in opposite directions [9]. The frequency at which the reflector produces waves is determined by the rate at which it encounters the wave crests from the source. For a wave group approaching the reflector in a left-handed medium, the wave crests are actually moving away from the reflector. Thus, the reflector encounters fewer (more) crests per second if it is moving towards (away from) the source than if it were stationary, resulting in a lower (higher) frequency of the reflected wave.

Magnetostatic spin waves travelling in a thin film magnetic material, saturated by a magnetic field along the direction of propagation, are known to have negative dispersion. That is, the phase velocity and group velocity are in opposite directions. Such waves are termed backward volume magnetostatic waves (BVMW) [10]. Stancil et al. previously observed the reverse Doppler effect in BVMW for the case where the receiver is moving relative to the source [8]. We report here the observation of a reverse Doppler effect for BVMW reflecting off of a moving target, namely a travelling surface acoustic wave. These results are interesting for both fundamental

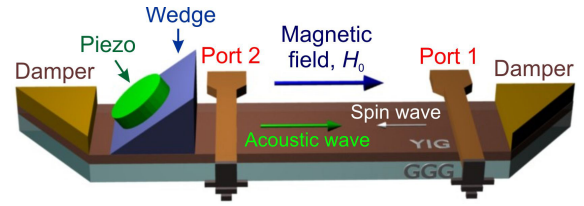


FIG. 1: (Color online) Experimental setup. Spin waves are excited and received in the YIG film by stripline antennae (Port 1 and Port 2). The SAW is excited on the YIG/GGG substrate by a piezoelectric quartz crystal and an acrylic wedge transducer.

research on linear and nonlinear wave dynamics, magnon-phonon interactions and for signal processing in the microwave frequency range. Microwave devices such as frequency shifters, adaptive matched filters and phonon detectors may be conceived using inelastic scattering of spin waves on acoustic waves.

The experiments were performed using 6 μm-thick yttrium iron garnet (YIG) films, which were epitaxially grown on 500 μm-thick, (111) oriented gadolinium gallium garnet (GGG) substrates. The substrates were cut into strips approximately 3 mm wide and 2 cm long. To produce the conditions for backward volume magnetostatic wave propagation, an external bias magnetic field of $H_0 = 1640$ Oe was applied in the plane of the YIG film strip along its length and parallel to the direction of spin-wave and SAW propagation (see Fig. 1). BVMW were excited and detected in the YIG film using microwave stripline antennae spaced 8 mm apart (shown as Port 1 and Port 2 in Fig. 1). The spin waves were generated by driving the antennae with the microwave source of a network analyzer (model Agilent N5230C). The microwave signal power, at 1 mW, was low enough to avoid non-linear processes. The microwave frequency was swept through the range 6.4–6.6 GHz. Simultaneously, surface acoustic waves were launched to propagate along

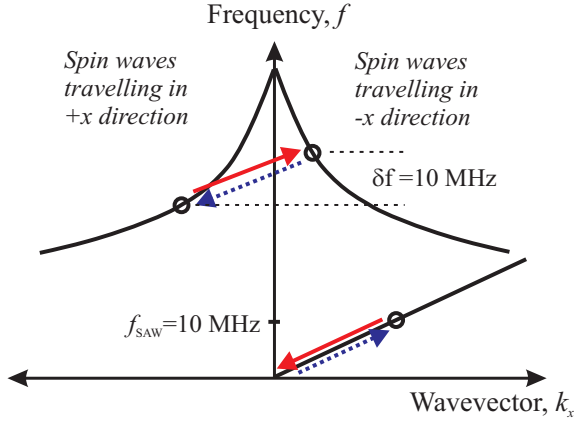


FIG. 2: (Color online) Schematic of dispersion curves for BVM SW and SAW. Circles indicate the waves that participate in Bragg scattering. Red solid arrows show the process of scattering of BVM SW on co-propagating SAW resulting in spin-waves shifted up in frequency while a phonon is annihilated. Blue dashed arrows show the process of scattering of BVM SW on counter-propagating SAW with the resulting spin-wave frequency shifted down while a phonon is generated.

the same path on the YIG/GGG sample. Longitudinal compressional waves at frequency $f_{\text{SAW}} = 10 \text{ MHz}$ were generated using a piezoelectric quartz crystal and coupled to surface modes in the YIG/GGG with an acrylic wedge transducer [11]. The wedge was machined to 51° form most efficiently transforming bulk acoustic waves into surface acoustic waves. A transformer and resonant circuit were used for impedance matching between the 50 Ω source and the piezoelectric crystal. The ends of the YIG/GGG sample were cut at a 45° angle and coated with a silicone acoustic absorber to avoid reflections (see Fig. 1).

The acoustic waves interact with the spin waves through the magnetostrictive effect in the magnetic material [12, 13]. The strain of the acoustic wave thereby periodically modulates the magnetic properties of the film, effectively producing a travelling Bragg grating of which the spin waves are reflected. Fig. 2 shows schematically the dispersion curves for both the BVM SW and SAW. One can see that the group velocity of BVM SW, as determined from the slope of the dispersion curve, is negative for positive wave vectors and vice versa. Thus, points on the BVM SW curve to the left of the axis represent waves propagating or carrying energy to the right from Port 2 to Port 1. Conversely, spin waves propagating to the left from Port 1 to Port 2 appear on the right side of the plot. The surface acoustic waves have a normal, linear dispersion relation: SAW travelling to the right from the prism are indicated by points on the right side of the plot.

The scattering process of spin waves on the acoustic waves must conserve energy and momentum. Fig. 2 shows schematically the transitions allowed by the con-

servation laws. The annihilation of a phonon (red solid arrows in Fig. 2) corresponds to the generation of a magnon of higher frequency and travelling in the opposite direction of the original spin wave. It is clear that for the experimental setup shown in Fig. 1, this interaction can be realized only for the spin wave which propagates in the $+x$ direction, i.e., in the same direction as the SAW. One can see that the Doppler effect is reversed since the reflected spin wave has higher frequency. Another process is realized with the generation of the phonon (blue dashed arrows in Fig. 2), which corresponds to the generation of a magnon of lower frequency travelling in the opposite direction of the original spin wave. This process takes place between counter-propagating spin and acoustic waves. The Doppler shift, δf , is equal to the SAW frequency in both cases.

Fig. 3(a) shows the experimentally measured BVM SW transmission characteristic for the YIG film as determined from the S_{21} parameter (power received at Port 2 relative to the power delivered to Port 1). The spin-wave transmission band is bounded above by the ferromagnetic resonance frequency and below by the antenna excitation efficiency. It has a maximum just below the point of ferromagnetic resonance ($f_{\text{FMR}} = 6577 \text{ MHz}$).

Fig. 3(b) shows the reflection characteristics for Port 1 (S_{11} parameter) due to spin waves generated at Port 1 being reflected back to the same antenna. The Doppler shifted frequencies were measured by tuning the network analyzer to detect signals at frequencies offset by plus and minus 10 MHz (i.e., $\pm f_{\text{SAW}}$) from the swept source frequency. Similarly, the reflection characteristics for Port 2 are shown in Fig. 3(c). In each case, the frequency axis is the swept source frequency.

One can see from Fig. 3(b) that both up and down-shifted frequencies exist for the reflected spin waves (P_+ and P_- signals in figure). The reason is as follows: with the microwave signal applied to Port 1, the antenna excites spin waves propagating outwards in both directions from the antenna. The spin waves propagating to the left, towards the acoustic source, encounter approaching surface acoustic waves and are partially scattered back towards the source antenna with a reverse Doppler shift down in frequency. The spin waves propagating to the right, away from the acoustic source, encounter receding acoustic waves and are scattered back with an up-shift in frequency due to the reverse Doppler effect.

The allowed transitions shown in Fig. 2 are equivalent to the Bragg reflection conditions. For frequencies meeting these conditions, the reflected spin wave power is maximized. Thus, the peaks in the P_+ and P_- curves correspond to the phonon annihilating up-shift and phonon generating down-shift processes respectively. The down-shift process must start at a higher spin wave source frequency and, in the reverse transition, the up-shift process must start from a lower original spin wave frequency. Thus, the difference in source frequency for the up-shift

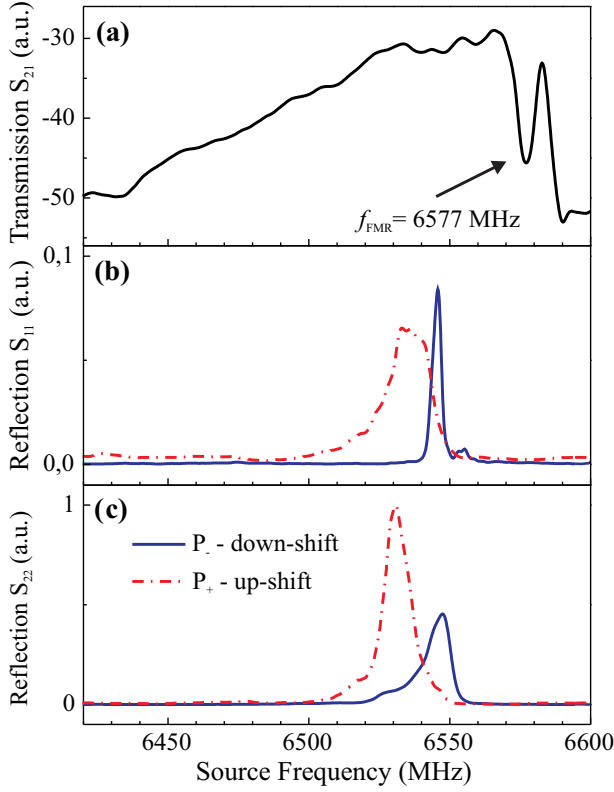


FIG. 3: (Color online) (a) BVM SW transmission characteristic for the YIG film. (b) and (c) The reflection characteristics for Port 1 and Port 2 respectively. The solid blue curve, P_+ , is for the detector frequency set 10 MHz below the source frequency. The dashed red curve, P_- , is for the detector frequency set 10 MHz above the source frequency. In each case, the frequency axis is the swept source frequency.

and down-shift process, f_- , should be equal to the SAW frequency, f_{SAW} . This is seen in the experimental results shown in Fig. 3 (b): the source frequency at which the P_+ signal reaches a maximum is 10 MHz lower as compared to the P_- signal. The peak of the down-shifted reflection is larger and narrower because the path length over which the acoustic and spin waves can interact is approximately two times longer on the left side of the antenna. Although both up-shifted and down-shifted signals are present in the experimental results, it is clear from the relative amplitudes that the up-shifted signal is due to the co-propagating waves, verifying the reverse Doppler effect.

The reflection characteristics for Port 2 are presented in Fig. 3 (c). One can see that for Port 2, the up-shifted reflection is stronger because the rightwards propagating spin waves (which reflect off of receding acoustic waves) have a longer interaction path length. Note the difference in the scale between Fig. 3 (b) and (c); the Port 2 signals are stronger because the acoustic amplitude is larger near the source. Similar to Port 1 results, the positions of the peaks differ by approximately f_{SAW} . The frequency

difference between the maxima in P_- and P_+ signals is $f_1 = 10$ MHz and $f_2 = 15$ MHz for Port 1 and Port 2 respectively. The discrepancy in f_2 from the expected 10 MHz is likely due to part of the interaction occurring under the wedge: here, the SAW wavelength differs from that in the unloaded YIG film. Thus, the spin wave frequencies at which the Bragg conditions are met are different for the co- and counter-propagating cases. It should be noted that the actual Doppler frequency shift in the reflected spin wave is exactly 10 MHz in both cases, as determined by the detector frequency offset.

To construct a simple and representative theoretical model, we consider the BVM SW dispersion relation to be nearly linear for small wavenumbers ($kd \ll 1$, where d is the thickness of the YIG film). Thus, we can write

$$f_{\text{SW}}(k) = f_{\text{FMR}} + v_{\text{SW}} k;$$

where

$$v_{\text{SW}} = \frac{f_H f_M}{4f_{\text{FMR}}} d$$

is the group velocity of BVM SW. Here $f_H = H_0$, $f_M = 4 M_0$, where $\gamma = 2.8$ MHz/Oe is the gyromagnetic ratio.

The dispersion relation for the SAW is nearly linear with $f_{\text{SAW}}(k) = v_{\text{SAW}} k$, where v_{SAW} is the phase and group velocity of the acoustic wave. Fulfilling laws of energy and momentum conservation by the transitions indicated in Fig. 2, a simple equation can be derived for the initial spin-wave frequencies f_+ and f_- which correspond to the maxima of P_+ and P_- :

$$f_{\pm} = f_{\text{FMR}} \pm \frac{f_{\text{SAW}}}{2} \left(\frac{v_{\text{SW}}}{v_{\text{SAW}}} \mp 1 \right)$$

Using saturation magnetization $4 M_0 = 1750$ G for the YIG film, BVM SW group velocity $v_{\text{SW}} = 3.2$ cm/s, and SAW velocity $v_{\text{SAW}} = 0.5$ cm/s this equation gives the values for $f_+ = 6537$ MHz and $f_- = 6547$ MHz which is in good agreement with the experimental data (see Fig. 3).

In conclusion, we have observed the reverse Doppler effect in backward spin waves reflected off of surface acoustic waves. Both possible situations were analyzed: the scattering of BVM SW from co-propagating and counter-propagating SAW. It was shown that the frequencies of scattered spin waves in both cases were shifted by the frequency of SAW according to the reverse Doppler effect. The results are in good agreement with the theoretical analysis based on the dispersion curves of spin waves and acoustic waves. Similar reverse Doppler effects are to be expected in other left-handed media.

This work was partially supported by the DFG SE 1771/1-1, and NSF ECCS 0645236. Special acknowledgments to Prof. G. A. Melkov for valuable discussions.

-
- [1] C. Doppler, Abh. Königl. Bohm. Ges. Wiss. 2, 465 (1843).
- [2] C. H. Papas, Theory of Electromagnetic Wave Propagation (McGraw-Hill, New York, 1965).
- [3] V. E. Pavlov, JETP, 36, 1853 (1959).
- [4] V. G. Veselago, FTT, 8, 3571 (1966).
- [5] N. Seddon and T. Bearpark, Science 302, 1537 (2003).
- [6] E. Reed, M. Soljacic, and J. Joannopoulos, Phys. Rev. Lett., 91, 133901 (2003).
- [7] K. Leong, A. Lai and T. Itoh, Microw. Opt. Tech. Lett., 48 545 (2006).
- [8] D. Stancil, B. Henry, A. Cepni, and J. Van't Hof, Phys. Rev. B, 74, 060404 (2006).
- [9] V. G. Veselago, Usp. Fiz. Nauk 92, 517 (1967).
- [10] R. W. Damon and J. R. Eshbach, Phys. Chem. of Solids 19 308 (1961).
- [11] S. Hanna, G. Murphy, K. Sabetfakhri, and K. Stratakis, Proc. Ultrason. Sym. 209 (1990).
- [12] S. M. Hanna and G. P. Murphy, IEEE Trans. Magnetics, 24, 2814 (1988).
- [13] Yu. V. Gulyaev and S. A. Nikitov, Sov. Phys. Solid State, 26, 1589 (1984).